Estimation of critical stress ranges to preserve soil functions for differently textured soils

---

Julia Pöhlitz[1]*, Jan Rücknagel[1], Steffen Schlüter[2], Hans-Jörg Vogel[2], Olaf Christen†[1]

[1] Martin Luther University Halle-Wittenberg, Department of Agronomy and Organic Farming Betty-Heimann-Str. 5, 06120 Halle/Saale, Germany

[2] Helmholtz Centre for Environmental Research GmbH – UFZ, Department of Soil System Sciences, Theodor-Lieser-Str. 4, 06120 Halle/Saale, Germany

*Corresponding author: Email address: julia.poehlitz@landw.uni-halle.de, phone: +49/3455522631, Address: Department of Agronomy and Organic Farming, Martin Luther University Halle-Wittenberg, Betty-Heimann-Str. 5, 06120 Halle/Saale

Research highlights

Mechanical precompression stress can be similar for different textured soils near field capacity.

Texture does not primarily determine the compaction sensitivity of soils.

X-ray CT provide valuable additional information about the effect of mechanical stresses.

Abstract

The use of heavy agricultural equipment often produces significant changes in soil physical properties through compaction. Soil compaction is one of the environmental factors in agriculture that adversely act on soil functions such as the provision of air, water, nutrients and pore space for root growth affecting crop yields.

In this study, critical stress values are defined as the values at which the effects of compaction result in a limitation of soil functions. Soil functions such as water storage, habitat and plant production are influenced to a different degree by soil compaction, so we assume there is not some fixed critical stress threshold for soil, but a range of critical stress values, hereafter called critical stress range. It is investigated, if there are differences in the critical stress values with respect to soil functions leading to critical loads that should not be exceeded to prevent negative effects, and if the critical stress ranges differ for different textures.

Using column experiments in a greenhouse classic soil mechanical parameters (dry bulk density, mechanical precompression stress), morphometric parameters obtained with X-ray tomography (macroporosity, pore connectivity) from undisturbed soil samples as well as biological parameters (earthworm activity) and crop factors (grain and straw yield) were investigated for soils with different topsoil textures (top soil 0-15 cm: loam, silty clay loam, silt loam, sandy loam) near field capacity.

We found that critical stress values for various parameters and critical stress ranges did not depend on topsoil texture at this matric potential. Studies, which recommend maximum values for mechanical loads to prevent harmful soil compaction solely based on texture, should be treated with caution. Although the soil textures at the four sites were quite different, the middle of the critical stress ranges were similar and concurred with the values of the mechanical precompression stresses which were similar at all four sites, too. The agronomic critical stress values of grain and straw yield mostly were impaired at the lower limit of the critical stress ranges and were, therefore, the most sensitive parameters.

Keywords: pre-compression stress; X-ray CT; soil compaction

Introduction

Plants use a soil as a growth medium, which supplies water, oxygen and nutrients. Agricultural soils are therefore conditioned to create a soil structure that allows optimal plant and root growth, optimal biological activity to release nutrients, and to facilitate the supply of water and oxygen (Carter, 1986). As a result of excessive machine loads as well as improper air pressure in the tires and tillage equipment, harmful soil compaction can occur (Pagliai et al., 2000; Rücknagel et al., 2012). This is especially true for unfavorable water contents during agronomic operations. Soil compaction is an undesirable change in soil structure (Ishaq et al., 2001) which influences not only pore functions such as air and water movement (Lipiec & Hatano, 2003), but also biological activity (Lipiec & Simota, 1994).

It is important to evaluate the changes of soil properties caused by soil compaction from different angles, (Horn & Rostek, 2000; Lipiec & Hatano, 2003), as will be outlined below. Lipiec & Hatano (2003) refer to soil properties including soil strength, aeration, water, and structural characteristics that make it easier to characterize soil quality after compaction. A key criterion for the soil's stability when subjected to mechanical loads is precompression stress, a property that is often used in soil mechanics (Horn & Rostek, 2000). Once it is exceeded irreversible changes in soil functions occur (Rücknagel et al., 2017). Macropores, typically defined for pore diameters >50 µm, constitute a comparatively small fraction of the total pore space, but can contribute substantially to total flow, especially at high water content and at high precipitation rates where they cause the phenomena of preferential flow. This is why physical disturbance of macropores caused by soil loading may lead to a significant reduction of hydraulic conductivity and air permeability as described by McKenzie et al. (2009). With a decreasing macroporosity, it can be assumed that larger air-filled pores become discontinuous causing limitations in oxygen supply. In a recent review, Rabot et al. (2019) highlight the relevance of the pore structure for the multitude of soil functions. Hence, it seems to be promising to complement classical methods by non-destructive imaging tools such as computed tomography to better characterize the structure of the pore network in quantitative terms (Jarvis et al., 2017; Pihlap et al., 2019; Pöhlitz et al., 2019). In agricultural systems, biological properties as well as physical or mechanical properties are important components of the soil ecosystem as pointed out by Carter (1986). He also advises that indices of both soil structure and biological conditions are important for understanding the behaviour of soil functions and, thus, the ability to avoid or recover from soil compaction. McKenzie et al. (2009) emphasize that earthworms are the major component of the soil fauna in temperate agro-ecosystems. Also Guei & Tondoh (2012) explain the important role of earthworms as soil "ecosystem engineers" brought by feeding, burrowing and forming habits in and between casts which maintain soil fertility and soil conservation (organic matter and macroaggregates). Soil compaction can gradually affect earthworm activity in soil (Ruiz et al., 2015). They can be sensitive to tillage techniques and can therefore be used as bio-indicators of soil conditions (Lemtiri et al., 2014). Besides soil fauna also plant growth can be a sensitive indicator for soil compaction. Czyz & Tomaszewska (2001) found that grain yield was linearly related to root mass, showing the importance of good soil physical conditions for root growth for optimal yields. Crop yields in compacted soils are usually associated with the extent and function of the root system (Lipiec & Hatano, 2003) which is impaired by decreasing root penetration due to excessive mechanical resistance (Lipiec & Simota, 1994), reduced infiltration and insufficient aeration (Czyz & Tomaszewska, 2001).

To evaluate the impact of soil compaction on soil functions it is of particular interest to know at what state of compaction soil properties such as dry bulk density, porosity or pore connectivity become critical. The reduction of a soil property with increasing load might be sharp or gradual. In the latter case the definition of a critical compaction status is difficult and typically set to empirically determined values based on the soil properties of interest like crop growth. Thereby, critical thresholds are expected to depend on climatic conditions, soil type and crop species (Rashid & Sheikh, 1977). Several studies examined dry bulk density (BD) as suitable indicator for critical soil compactions since high BD has been considered limiting for soil aeration and rooting (O'Connell, 1975). More specifically, an air capacity, i.e. air-filled porosity at field capacity, of less than 10 %

was found to be limiting for crop growth (Lebert et al., 2004; O'Connell, 1975; Reichert et al., 2009; Werner & Paul, 1999) and the corresponding bulk density at which this occurs was determined by regression equations that also take organic matter, particle density and combined silt and clay content into account. Kaufmann et al. (2010) list optimal and limiting values for dry bulk density derived from parabolic relationships between dry bulk density and crop yield which show a pronounced maximum depending on soil conditions, crop species and climate.

Focusing on only one soil property is problematic because it is possible that one soil property is optimal, while another already shows critical values. The questions arise, whether the soil functions mentioned above react differently to soil compaction, i.e. become limiting at the same applied stress, and whether there are texture dependent differences. In this study, critical stress values are defined as the values at which the effects of compaction result in a limitation of soil functions. Soil functions and their parameters are influenced to a different degree by soil compaction, so we assume there is no fixed critical stress threshold for a given soil, but a range of critical stress values, hereafter called critical stress range. We investigate the influence of soil texture on changes in some key properties which are deemed important for different soil functions. Classic soil mechanical parameters and macropore characteristics derived from X-ray CT (undisturbed samples) as well as biological and plant parameters (number of biopores, grain and straw yield) are linked. The aim is to explore if there are differences in the critical stress values for the different parameters, and if the critical stress ranges differ for different textures in topsoil near field capacity. We chose field capacity because this corresponds to the field conditions when mechanical loading typically occurs, namely high water content in the spring after the winter melt for sowing and in late autumn for harvesting. We are aware that the strength of a soil can increase with increasing drought (Pöhlitz et al., 2019; Rücknagel et al., 2012). This study should provide extended insights into the topsoil compaction process and structural characteristics of different soil textures near field capacity, and contribute to a suitable management of soils so that soil physical, morphological, biological and plant parameters are not adversely affected by soil compaction.

2. Material and Methods

2.1. Data acquisition

In autumn 2016 soil samples were taken from the topsoil (0-20 cm) of four differently textured sites (loam, silty clay loam, silt loam, sandy loam) which were specifically selected to represent a wide range of soil textures. The clay content varies between locations from 70 g kg^{-1} to 280 g kg^{-1}. The sand contents are between 40 g kg^{-1} and 530 g kg^{-1}. At all sites, long-term reduced tillage (FAO, 1993) took place with cultivator. An overview and description of the locations is given in Table 1.

2.2. Soil physical measurements

For the soil physical investigations undisturbed samples (volume = 250 cm^3, height = 6.1 cm, internal diameter = 7.2 cm) were taken in three repetitions at five places per site (3 x 5 x 4 = 60).

The saturated hydraulic conductivity (K_s, cm d^{-1}) of the soil samples (volume = 250 cm^3, height = 6 cm) was measured by means of a stationary system (Klute & Dirksen, 1986) with a flow duration of 4 h. The dry bulk density (BD, Mg m^{-3}) of the same samples was subsequently determined from the dry weight after drying at 105°C for 48 h (Blake & Hartge, 1986).

2.3. Soil mechanical measurements

For soil mechanical measurements undisturbed soil samples (volume = 220 cm^3, height = 2.8 cm, diameter = 10 cm) were taken at four places per site (4 x 4 = 16). The shallow sample geometry was dictated by subsequent oedometer measurements (see below). For the compression tests eight load steps (5, 10, 25, 50, 100, 200, 350 and 550 kPa) were applied to each soil sample.

The soil samples were first slowly saturated by capillary rise before being drained for at least seven days in a sandbox with a hanging water column to a matric potential of -6 kPa (Klute, 1986) and then weighed.

Fully automated oedometers and the associated software (WINBOD32, Wille Geotechnik, APS Antriebs-, Prüf- und Steuertechnik GmbH, Göttingen-Rosdorf, Germany) were used to determine the stress - strain relationships under drained conditions. Load application was uniaxial. Each load step was applied with a load time of 120 min and a subsequent relaxation time of 15 min with a 2 kPa load. The oedometer records settlement with an accuracy of 0.01 mm.

After the compression tests, the soil samples were dried at 105°C for 48 h and then weighed (Blake & Hartge, 1986). The dry mass was then divided by the initial sample volume to compute the dry bulk density prior to the compression tests (BD_0). Using the settlement (s), the initial height of the soil sample (h_0), and BD_0 the resulting BD after each load application (BD_{xi}) was calculated as follows:

$$BD_{xi} = BD_0 \cdot \frac{h_0}{h_0 - s} \tag{3.1}$$

A semi-logarithmic stress - BD_{xi} curve was then created. The mechanical precompression stress was determined based on these curves using the graphical method of Casagrande (1936). It was applied by a number experimenters to minimize subjectivity (Rücknagel et al., 2010).

2.4. CT examinations

An X-ray CT scan was acquired after each load step (App. 1). Soil samples from the compression tests were scanned with an energy of 150 kV and a beam current of 550 µA using an industrial X-ray scanner (X-Tek XTH225, Nikon Metrology). One scan comprised 2480 projections with an exposure time of 1.41 s (scanning time was 2480*1.42s = 3500 s). A CCD detector panel with 2000×1750 diodes recorded the projections. Beam hardening artifacts were reduced with a 0.1 mm copper filter. The CT scans were reconstructed with a spatial resolution of 60 µm and an 8-bit greyscale resolution using the X-Tek CT Pro software package (Nikon Metrology). This is the maximum resolution, which allows to scan the entire sample (10 cm in diameter) and to get representative CT images. The results therefore pertain to pore sizes larger than 60 µm, but can only detect pores larger than two-three voxels faithfully (Vogel et al., 2010). Image processing was performed with the Java software ImageJ 1.50e (Rasband, 1997-2015). To reduce scatter and noise the CT scans were filtered using the "Non-local Means Denoising" plugin in Fiji (Buades et al., 2005).

In order to exclude artefacts at the edges of the sample and reduce the data volume a cylindrical region of interest (ROI) with a diameter of 90 mm was used in the middle of the reconstructed CT scan. The vertical extent of the ROI was adjusted to the reduction in sample height after each load step. This was based on the positions of small and identifiable features, e.g. stones, at the upper and lower ends of the sample. Regardless of compaction status it was thus always possible to locate the original soil volume again after each consecutive load application.

Automatic segmentation was then applied to the scan of the ROI to separate the image into pores and soil matrix. This was carried out using the thresholding method by Otsu (1979). Macroporosity (here pore diameter > 60 µm) was quantified as the ratio of the number of pore voxels to the total number of voxels within the ROI. The ImageJ analysis "Particle Analyzer" (Ferreira & Rasband, 2010-2012) was employed to calculate pore connectivity, which represents the connection probability between two arbitrarily chosen pore voxels, i.e. the chance to belong to same pore cluster. This dimensionless number is also denoted as the Γ indicator (Renard & Allard, 2013; Schlüter et al., 2014) and has a value between 0 and 1, where the latter indicates that the soil pores are perfectly connected.

2.5. Soil biological and agronomic measurements

Column preparation

Sufficiently large soil volumes are required for soil biological and agronomic measurements to minimize the impact of wall artifacts. Undisturbed soil cores of such size could not be extracted in the field. Therefore, a total of approximately 750 kg of disturbed soil from 0-20 cm depth was taken from each site (~750 kg x 4 = 3000 kg) to set up greenhouse experiments with repacked soil at different compaction levels. For the column experiments with earthworms (*Lumbricus terrestris*) and for the column experiments with spring barley (*Hordeum vulgare*) six dry bulk densities were produced in five repetitions for each site (6 x 5 x 4 = 120 columns). For both column experiments, the columns were positioned in a randomized order. The two column experiments took place independently of each other.

Opaque polyvinyl chloride (PVC) pipes were used for the column experiments (19 cm inside diameter, 283.52 cm^2 surface area, 30 cm height). For each site it was tested in advance how far the soil was compactable which depends on soil texture. This was done by compacting the loose soil piece by piece in a 5 cm layer. In the end, we used the soil mass to calculate the final density. This final density corresponds to the highest density we were able to produce in the laboratory. From this density, which was different for each test site, we produced 5 further densities in steps of 0.07 Mg m^{-3}. Also, we compared these highest densities with the values that resulted from the stress strain tests. These corresponded to each other. Thus, for the four sites dry bulk density ranges of 1.42-1.77 Mg m^{-3} (loam), 1.28-1.63 Mg m^{-3} (silty clay loam), 1.21-1.56 Mg m^{-3} (silt loam) and 0.72-1.07 Mg m^{-3} (sandy loam) were produced.

The soil was manually compacted at a water content near field capacity directly after soil sampling using metal plates. To get the first layer a pre-weighed amount of soil was filled into a column and beaten until its volume was reduced to the required extent (5 cm). The second layer was then filled onto the compacted first layer in the column and treated in the same manner, and so on, until all the pre-weighed soil was filled into the column. In the columns representing a given site the same soil mass was used for all six dry bulk densities. This resulted in decreasing filling heights with increasing dry bulk density. The soil mass was chosen to yield a maximum filling height of 25 cm at the lowest dry bulk density. Using the same soil mass entails the same amount of nutrients in each column representing the same field site.

On the inside of the columns a duct tape which reached about 2.5 cm thickness into the column was attached after the second (10 cm), third (15 cm) and fourth (20 cm) layer counting from the top. This was done to prevent earthworms from crawling and plant roots from growing preferentially along the column wall.

Biological measurements

The earthworm genus *Lumbricus terrestris L.* was used for column experiments. In each column, six earthworms were placed on the soil surface. To prevent soil drying while permitting gas exchange (O_2), 30 g of wheat and oat straw about 5 cm in length was mixed together and placed on each surface. The upper end of the columns was covered with gauze and the lower one with a fleece to prevent the earthworms from escaping. The experimental conditions were constant darkness at 20°C. The total burrowing period of *L. terrestris* was 18 days.

After the experiment, the straw was carefully removed and collected by hand, together with the earthworm casts on the soil, to make the earthworm burrows visible on the surface. The biopores were counted at the top (0 cm), after the second (10 cm), third (15 cm), fourth (20 cm) and bottom layer (25 cm) of the columns, summed up, divided by the number of counted layers and converted to number per square meters representing average biopore activity of the first 25 cm topsoil in field.

Agronomic measurements

For the agronomic investigations, summer barley (*Hordeum vulgare L.*) of the variety Avalon was used. In each column, 15 plants were sown, covered with a roughly 3 cm thick soil layer of the same soil, and thinned to ten plants after emergence. For nitrogen, a target value of 90 kg N ha^{-1} was adjusted. N_{min} was determined (Tab. 1) and subtracted from the target value to obtain the amount of nitrogen to be applied to the surface of the columns in the form of calcium ammonium nitrate parallel to sowing.

The bottom of each column was covered with a fleece to prevent roots from growing out of the column. The columns were weighed regularly every few days to monitor water loss by evapotranspiration. This loss was then compensated by watering so that lack of water did not restrict plant growth.

The experiments were carried out in a greenhouse with the climatic conditions regulated according to the BBCH stages of cereals (Witzenberger et al., 1989) as follows: (i) germination, leaf development and tillering: constant 15°C with a 12 h photoperiod; (ii) stem elongation and booting: 20°C during the day and 15°C at night with a 14 h photoperiod; (iii) inflorescence emergence, heading, flowering, anthesis, development of fruit, ripening and senescence: 25°C during the day and 20°C at night with a 15 h photoperiod. The total growing period of the crop was 130 days.

At the senescence stage, the plants were harvested 1 cm above the soil. Straw and grain were dried separately at 105°C to a constant weight, which was then converted into a yield (g m^{-2}).

2.6. Derivation of critical stress values and critical stress ranges

Critical stress values and critical stress ranges

With precompression stress and CT-derived parameters we target the critical stresses were transitions in the properties are strongest or reach absolute thresholds, whereas for biopores and yield we target optimum values, i.e. where the onset of detrimental effects by compaction occur. We think that this is justified by the fact that the former are soil inherent properties, whereas the later reflect emerging biological behavior constrained by the present soil structure. The respective minimum and maximum spread have been added to the critical stress values. The critical stress range is between the lowest and highest critical stress value of the examined parameters for each soil.

Mechanical precompression stress

The mechanical precompression stress is widely viewed as the most important measure to assess harmful soil compaction. Hence, it is used here as a critical stress value for the mechanical component of a soil (section 2.3.).

Macroporosity

According to Werner & Paul (1999) an air capacity of ≥ 8 Vol.-% at pF1.8 (pores > 50 µm) is necessary to maintain the ecological functionality of cohesive soils. Air capacity, when measured at this matric potential, can be considered equivalent to macroporosity (Drewry et al., 2008). Here, macroporosity was determined with CT quantitative image analysis at a similar resolution (pore size). Following Werner & Paul (1999) a macroporosity ≥ 8 % was considered to be the minimum required. So, as soon as a macroporosity of 0.08 was reached, the corresponding stress value was considered to be the critical stress value.

Pore connectivity

There are no critical values given in the literature regarding pore connectivity, i.e. for the collapse of a well-connected pore network into many isolated pores. In this study, the first significant change in connectivity with increasing load application is therefore considered the critical stress value.

Biopores, Grain & Straw yield

For the relationship between dry bulk density and yield an optimal dry bulk density at maximum yields is frequently reported (Czyz & Tomaszewska., 2001, Czyz, 2004). Since we noted that the volume of biopores is directly related to bulk density, we assumed, just as described with the yield, that an optimal dry bulk density also leads to maximum biopore numbers. BD_{opt} is then used to derive the critical stress value with the help of the stress - BD_{xi} diagram as follows (Fig. 1): BD_{opt} is targeted on the abscissa of the BD – Biopores or BD – yield diagram. Then the critical stress value at which BD_{opt} value is reached can be read of the ordinate of the stress - BD_{xi} diagram. At lower BD there is little burrowing activity, because there is less need to dig to obtain food and shelter or there is bad soil root contact (Kemper et al., 1988; Shah et al., 2017; Stovold et al., 2004). At higher BD burrowing is mechanically restricted or there is a high mechanical resistance to root penetration and reduced availability of oxygen, water and nutrients (Daddow & Warrington, 1983; Håkansson, 1989; Saqib et al., 2004).

2.7. Statistical analyses

The statistical analyses were carried out with the statistics program 'R Studio' (version 0.99.893, R Foundation for Statistical Computing).

The arithmetic mean values for BD_{xi}, macroporosity, pore connectivity, biopores density and crop yield were calculated separately for the repetitions of each site. The means of the log-normally distributed saturated hydraulic conductivity and precompression stress values were calculated based on the logarithmized values. For the variance analyses, all parameters were tested for normal distribution (Shapiro-Wilk test) and variance homogeneity (Levene's test).

A one-way analysis of variance was performed for all parameters between sites within each load step, and between the eight load steps of the compression tests and between the six dry bulk densities from the column experiments for each location separately. The Tukey honestly significant difference test was applied to determine differences in group means and was considered significant at a significance level of $p \leq 0.05$.

3. Results

3.1. Soil mechanical parameters and accompanying critical stress values

The stress - BD_{xi} diagrams (Fig. 2) show classic compaction curves for each of the four sites. The BD_{xi} curves for the four sites run more or less parallel, but are shifted up or down with respect to their initial densities, where the loam site had the highest and the sandy loam site the lowest density. The values of the mechanical precompression stress ($\sigma_{P\ BDxi}$) determined from the stress - BD_{xi} diagrams do therefore not differ significantly between the sites. They are in the range of log σ_P = 1.65 to 1.85 (45 to 71 kPa).

The increase in load results in significant decreases in macroporosity (Fig. 3) and pore connectivity (Fig. 4), regardless of the site. Only at the lowest load steps, did the loam and silt loam sites on the one hand, and the silty clay loam and sandy loam sites on the other differ significantly from each other in terms of macroporosity and pore connectivity (App. 2). Because of different initial dry bulk densities, the loam, the silt loam and the sandy loam site have lower macroporosity and pore connectivity values than the silty clay loam site.

The stress - macroporosity curves (Fig. 3) show the most significant decrease in macroporosity in the load range between 25 and 200 kPa. At the highest load steps (350 to 550 kPa) macropores disappeared almost completely. This is true for all four sites. The macroporosity at the loam site can already be regarded as critical (<0.08) at a load of 12 kPa (Fig. 3A). At the silty clay loam site

(Fig. 3B) the critical stress value for macroporosity is reached at a much higher load of 155 kPa. The silt loam (Fig. 3C) and sandy loam (Fig. 3D) sites have a critical stress value for macroporosity of 52 and 72 kPa, respectively, which is near the value for the mechanical precompression stress for these two sites.

The shape of the stress - pore connectivity curves (Fig. 4) for all sites is similar to that of the stress - macroporosity curves, with the difference that pore connectivity remains more constant with increasing load for a longer time before decreasing steeply in the load range of 50-200 kPa. In all soils a significant reduction in connectivity happened at a load of 100 kPa except for the silt loam site (Fig. 4C) where this ad-hoc definition of a critical stress value for pore connectivity occurred at 200 kPa. This is in contrast to other soils where the collapse of connectivity happened already at a load of 100 kPa.

3.2. Soil biological parameters and accompanying critical stress values

L. terrestris dug successfully into the soil in all columns, even at the highest dry bulk densities. Mortality was negligible and was not related to BD. *L. terrestris* formed permanent continuous burrows with little branching. Several individuals of *L. terrestris* in a column sometimes used the same burrow system. This means not every earthworm dug a biopore. The shape of the biopores was affected by the compaction procedure which led to a series of layers with a slightly higher bulk density in the upper part as compared to the lower. Interestingly, *L. terrestris* tended to follow the less compacted zone on top of each layer so that the burrows in those areas were horizontal. This was especially observed at the maximum burrowing depths. But this peculiarity did not affect the estimated number for biopore density. There were biopores even at the lower end of some lower density columns.

For all soils, except for the loam, the density of biopores slightly increased with increasing bulk density before it declined above some optimal bulk density (Fig. 5B-D). For the loam soil no effect of BD on the number of biopores was observed (Fig. 5A, App. 3). In this case the critical stress value of 11 kPa was set at BD_{xi} = 1.42 Mg m^{-3} where the mean biopore density was obtained.

To determine an optimal BD with respect to the burrowing activity of earthworms a polynomial could be fitted reasonably well to the measures biopore densities except for the loam (Fig. 5B-D). We used the maximum value of the fitted polynomials to determine the optimal BD and critical load which led to 1.40 Mg m^{-3}/80 kPa, 1.35 Mg m^{-3}/43 kPa and 0.82 Mg m^{-3}/20 kPa for the silt clay loam, silt loam and sandy loam respectively.

3.3. Agronomic parameters and accompanying critical stress values

For the silt loam and sandy loam soil grain yields increased with increasing bulk density (Fig. 6, App. 3) before it decreased again after an optimal bulk density was exceeded. For the loam and silty clay loam soils, grain yields decrease already with the first investigated reduction in bulk density. The loam (Fig. 6A) and silty clay loam (Fig. 6B) have the largest amplitudes in grain yields. Correspondingly, the graphs of the polynomial functions are steeper than those for the silt loam (Fig. 6C) and sandy loam (Fig. 6D) sites. For the latter two soils, no significant differences in grain yield with increasing density are found.

To determine an optimal BD with respect to the grain yield a polynomial could be fitted reasonably well to the measures grain yield densities except for the silt loam (Fig. 6A-D). We used the maximum value of the fitted polynomials to determine the optimal BD and critical load which led to 1.39 Mg m^{-3}/7 kPa, 1.30 Mg m^{-3}/45 kPa, 1.36 Mg m^{-3}/50 kPa and 0.89 Mg m^{-3}/56 kPa for the loam, silt clay loam, silt loam and sandy loam respectively.

In principle, the results for grain yield are reflected in the results for straw yield, with the difference that more straw was formed than grain, which led to shifts in the optimum density values (Fig. 7).

The maximum straw yield occurs at a density of 1.47 Mg m^{-3} for loam (Fig. 7A), 1.31 Mg m^{-3} for silty clay loam (Fig. 7B), 1.35 Mg m^{-3} for silt loam (Fig. 7C), and 0.87 Mg m^{-3} for sandy loam (Fig. 7D). This corresponds to critical stress values of 30 kPa for loam, 48 kPa for silty clay loam, 43 kPa for silt loam, and 50 kPa for sandy loam. Again, for the last three sites the derived critical stress values for straw yield are in the range of the mechanical precompression stresses.

3.4. Critical stress ranges

The critical stress values given in chapters 3.1 to 3.3. are summarized in Figure 8. The minimum and maximum stress values for each soil determine the critical stress range, indicated by dotted vertical lines. The critical stress ranges differ between the soils. While the stress range is rather large for the loam, it is similar and much narrower for the silty clay loam, silt loam and sandy loam.

For the relations between individual critical stress values some general trends can be derived. The spread of the mechanical precompression stress are very small for all four soils. For most of the soils the critical stress value for macroporosity is smaller than the one for pore connectivity. The critical stress values for the biopores, grain and straw yield are usually in the lower part of the critical stress ranges.

4. Discussion

4.1. General remarks

Before looking at the critical stress values and critical stress ranges resulting from soil compaction the effects of compaction on the examined soil functions observed here should be briefly discussed.

- The initial BD's for the four sites were much lower than site-specific plant root limiting BD´s according to Kaufmann et al. (2010). Furthermore, the K_s values were much higher than the minimum rate recommended by Werner & Paul (1999). Hence, the soil structures were intact at all sites.
- Despite different initial densities, all stress - BD_{xi} curves showed a similar shape. The individual curves were merely shifted somewhat along the ordinate. Therefore, the values for the mechanical precompression stress were similar.

- For soils with low initial macroporosity the critical stress value for macroporosity is smaller than the one for pore connectivity, whereas the values are similar for soils with high initial macroporosity. This discrepancy is caused by the different criteria of how critical stress values are determined for both properties. For macroporosity absolute values are considered (threshold at 0.08), whereas for pore connectivity relative differences mattered (significant changes between consecutive load steps). This also restricted critical stress values to actual measured load steps as no interpolation is possible. In the future the method could be changed to an absolute threshold of 0.5. It has been shown frequently that pore connectivity drops in a narrow macroporosity range of 5-10% (Jarvis et al., 2017; Pihlap et al., 2019; Pöhlitz et al., 2019). This also explains the empirical air capacity limit of about 8 % by volume in Werner & Paul (1999), because then the air-filled pore space becomes discontinuous and the oxygen supply is disturbed. Even if the mechanical precompression stress is exceeded, the macropores are still connected.
- Several individuals of *L. terrestris* shared biopores. This is in agreement with the studies of Jegou et al. (1998) and Joschko et al. (1989).
- The burrowing activity of *L. terrestris* varied with dry bulk density, following a parabolic curve except for the loam site. At low BD there was little burrowing activity, because there is less need to dig to obtain food and shelter. Up to a certain point (optimal BD) the number of burrows increased with increasing soil density. Beyond this point the burrowing activity decreased with BD, because *L. terrestris* was mechanically restricted, i.e. soil strength seemed to be a limiting factor at higher densities. A lower burrowing rate at higher densities was also found by Kemper et al. (1988) and Stovold et al. (2004). Schrader et al. (2007) and Kemper et al. (1988) observed that *L. terrestris* failed to penetrate a silt loam soil with a BD of 1.60-1.70 Mg m^{-3}. Similarly, Horn (1999) named 1.67 Mg m^{-3} as the BD limit for *L. terrestris*.
- We observed that at high soil densities, *L. terrestris* tended to remain in a particular location. Perreault & Whalen (2006) also reported such a behaviour, if *L. terrestris* was exposed

to unfavorably cold and wet soil conditions. Recall that in this study, the soil was at 20°C and moist, i.e. the conditions were favorable.

- Very loose (bad soil root contact) as well as heavily compacted soil (high mechanical resistance to root penetration, reduced availability of oxygen, water and nutrients) leads to reduced yields, as found by Daddow & Warrington (1983), Håkansson (1989), Saqib et al. (2004) and Shah et al. (2017), too.
- The parabolic relationship between dry bulk density and burrowing activity of *L. terrestris* as well as grain and straw yield of *H. vulgare* depends on texture. The optimal BD and the steepness of the curve differ.
- It seems that an increased content of organic matter like at the sandy loam site (51 g kg^{-1}) only has an effect on the dry bulk density of a soil, but not on the other parameters studied here.
- The mechanical precompression stress reflects critical stress value for yield or critical stress ranges in general.

4.2. Critical stress ranges

In this study, critical stress values for various parameters in topsoil near field capacity were presented. Single values were taken from fitted curves. However, in some cases, the curves were fairly flat and the data had a high standard deviation. Consequently, it is possible to pick a number of plausible critical stress values for a given parameter. For some the possible critical stress values have a rather big spread, for example the critical stress value for biopores at the loam site. This is because biopore density is insensitive to dry bulk density. Overall, for grain and straw yield the spread among soils is widest.

The values for the mechanical precompression stress at the four sites are fairly similar. The spread is the lowest for all parameters. In general, the mechanical precompression stress lies in the middle of the critical stress ranges for the other five investigated parameters and covers them reasonably well.

The critical stress value for biopores, usually appeared at the lower part of the critical stress range. For the loam site, one can assume that the critical stress value is very low due to the high sand content, because the rough surface of the sand particles can impair burrowing activity (McKenzie et al., 2009). At higher dry bulk densities this effect may increase, because the particles move closer together, which further increases friction (Horn et al., 1995). However, with increasing dry bulk density no significant differences of biopore number could be determined. This could be attributed to the lack of aggregation (Beisecker et al., 1994) and the accompanying evenly distributed resistance. That may be why the earthworms were still able to burrow through the soil even after the mechanical precompression stress was exceeded. For the sandy loam site, the high content of organic matter compensates the aforementioned effect of a high sand content, because it ensures a loose and thus easily penetrable packing. In general, the dry bulk densities were low so that there was little burrowing resistance.

The critical stress value for grain yield is very close to the one for straw yield. The loam soil seems to be an exception to this but generalizations are difficult due to large spread in the data. Grain and straw yield tend to become critical before the mechanical precompression stress is reached. If one looks at the spread, grain and straw yield seem to be the most sensitive parameters and form the lower limit of the critical stress range. This is because they are determined at the bulk density of optimal growth and not at the bulk density of steepest decrease in some property, e.g. pore connectivity. Iler & Stevenson (1991) report that sandy soils have high growth-limiting dry bulk densities of around 1.65-1.75 Mg m^{-3}, but that plants already show a significant reduction in growth before those densities are reached. In addition, plants differ in their tolerance of soil compaction affecting germination and growth of some species but not others (Skinner et al., 2009). Ultimately, grain and straw yield are the most important parameters for the farmer.

Following these explanations it is not surprising that at different sites the critical stress value for a given parameter may lie at the upper or lower end of the critical stress range for all parameters considered here, and that its value and spread may differ between sites. For example, the critical stress range is widest at the loam site and narrowest at the silty clay loam site. However, if the middle of the critical stress ranges (recall the logarithmic scale) are looked at, it can be seen that they are similar in value (50 - 100 kPa), and also similar to the values of the mechanical precompression stresses (45 - 71 kPa). Hence, the mechanical precompression stress turns out to be well suited as a measure of the critical stress values and the critical stress ranges. Nevertheless, useful additional information about the effect of mechanical stresses on the soil structure is gained from considering the other parameters as well.

The results show that topsoil texture does not determine the compaction sensitivity near field capacity alone or at least not primarily. Field capacity has an important role because at this point the soil is most susceptible to compaction and corresponds to the field conditions when mechanical loading typically occurs, namely high water content in the spring after the winter melt and in late autumn for sowing and harvesting. Furthermore, this moisture level is the closest state of the aggregates for clay soils, which we have at the Buttelstedt site. However, of course the relationship between precompression stress and soil moisture (matric potential) is different for different soil textures – clay is very weak when wet but becomes very hard when dry, while sandy soils will not show as much change with initial matric potential (Schjønning & Lamandé 2018).

5. Conclusions

In this study we found that critical stress with respect to soil functions does not depend on soil texture. This can be concluded from a number of physical and biological soil characteristics (mechanical precompression stress, macroporosity, pore connectivity, number of biopores, grain and straw yield) which are known to reflect soil functions and which were measured after applying increasing mechanical loads for differently textured topsoils near filed capacity. This means that studies, which recommend maximum values for mechanical loads to prevent harmful soil compaction solely based on texture, should be treated with caution.

Based on the different soil characteristics we could identify critical stress ranges which slightly differ between the soils. However, despite the considerably contrast in soil texture, the centers of the determined stress ranges were similar and concurred with the values of the mechanical pre-compression stresses which were similar for all four soils. Hence, the mechanical precompression stress was confirmed to be a suitable measure of the critical stress values and the critical stress ranges. Nevertheless, useful additional information is gained from considering the other characteristics as well. The critical stress values for indicators of plant growth (i.e. grain and straw yield), were mostly found at the lower limit of the critical stress ranges meaning that plant growth is most sensitively affected by soil compaction.

Acknowledgments

Many thanks to K. Marschall of the “Thüringer Landesanstalt für Landwirtschaft”, S. Reimann of the “Thüringer Lehr-, Prüf- und Versuchsgut GmbH”, S. Ulrich of the „Quellendorfer Dienstleistungen AG & Co. OHG“ (Quellendorfer Landwirte GbR) and F. Mörseburg of the “Agragenossenschaft Großrudestedt” for their permission to take soil samples at their experimental sites in Quellendorf, Buttelstedt and Kranichborn. The expert technical assistance and guidance of J. M. Köhne in CT image acquisition is also gratefully acknowledged.

References

Arvidsson, J, Keller, T., 2004. Soil precompression stress: I. A survey of Swedish arable soils. Soil Till. Res. 77, 85-95.

Beisecker, R., 1994. Einfluss langjährig unterschiedlicher Bodenbearbeitungssysteme auf das Bodengefüge, die Wasserinfiltration und die Stoffverlagerung eines Löß- und eines Sandbodens. Bodenökologie und Bodengenese 12.

Berli, M., Kirby, J., Springman, S., Schulin, R.. 2003. Modelling compaction of agricultural subsoils by tracked heavy construction machinery under various moisture conditions in Switzerland. Soil Till. Res. 73, 57–66.

Blake, G.R., Hartge, K.H., 1986. Dry bulk density. In: Klute, A. (Ed.), Methods of soil analysis. Part 1: Physical and mineralogical methods, 2nd edition. American Society of Agronomy Monograph No. 28, Madison, Wisconsin, USA, pp. 363–382.

Buades, A., Coll, B., Morel, J.M., 2005. A review of image denoising algorithms, with a new one. Multiscale Model. Simul. 4, 490-530.

Carter, M. R., 1986. Microbial biomass as an index for tillage-induced changes in soil biological properties. Soil Till. Res. 7, 29-40.

Casagrande, A. 1936. The determination of the pre-consolidation load and its practical significance. Proceedings of the International Conference on Soil Mechanics and Foundation Engineering, Vol. III, pp. 60–64. Harvard University, Cambridge, Massachussets, USA.

Czyz, E. A., 2004. Effects of traffic on soil aeration, dry bulk density and growth of spring barley. Soil Till. Res. 79, 153–166.

Czyz, E. A., Tomaszewska, J., Dexter, A. R., 2001. Response of spring barley to changes of compaction and aeration of sandy soil under model conditions. Int. Agrophysics 15, 9–12.

Daddow, R.L., Warrington, G.E., 1983. Growth-limiting soil bulk densities as influenced by soil texture. WSDG Report TN-00005. USDA Forest Service, Watershed Systems Development Group, Fort Collins, Colorado, USA.

Dewry, J.J., Cameron, K.C., Buchan, G.D., 2008. Pasture yield and soil physical property responses to soil compaction from treading and grazing – a review. Aust. J. Soil Res. 46, 237–256.

Diserens, E., 2009. Calculating the contact area of trailer tyres in the field. Soil Till. Res. 103, 302–309.

FAO, 1993. Soil tillage in Africa: needs and challenges. FAO Soils Bulletin No. 69. FAO, Rome, Italy.

FAO, 1998. World Reference Base for Soil Resources. ISSS–ISRIC–FAO. World Soil Resources Report No. 84, Rome, Italy.

Ferreira, T., Rasband, W.S., 2010-2012. “ImageJ user guide - IJ 1.46”, im-agej.nih.gov/ij/ docs/guide/

Gee, G.W., J.W. Bauder. 1986. Particle-size analysis. In: Klute, A. (Ed.), Methods of soil analysis. Part 1: Physical and mineralogical methods, 2nd edition. American Society of Agronomy Monograph No. 28, Madison, Wisconsin, USA, pp. 383–411.

Guéi, A.M., Tondoh, J.E., 2012. Ecological preferences of earthworms for land-use types in semi-deciduous forest areas, Ivory Coast. Ecol. Ind. 18, 644-651.

Håkansson, I., 1989. Compaction of the plough layer-which degree of compactness is the best? Swedisch Univ. Agric. Sci., Uppsala. Fakta/markväxter 1, 4.

Horn, R., 1999. Verdichtung von Böden – Überlegungen zum Prozess und zur Prognose der mechanischen Belastbarkeit. Wasser und Boden 51, 9–13.

Horn, R., Domzal, H., Slowinska-Jurkiewicz, A., van Ouwerkerk, C., 1995. Soil compaction processes and their effects on the structure of arable soils and the environment. Soil Till. Res. 35, 23–36.

Horn, R., Rostek, J., 2000. Subsoil compaction processes – state of knowledge. Advances in GeoEcology. Reiskirchen, Catena, 32.

Iler G.S., Stevenson C.K., 1991. The effects of soil compaction on the production of processing vegetables and field crops. A review. Ridgetown College of Agricultural Technology, Ontario.

Ishaq., M., Hassan, A., Saeed, M., Ibrahim, M., Lal, R., 2001. Subsoil compaction on crops in Punjab, Pakistan. I. Soil physical properties and crop yield. Soil Till. Res. 59, 57–65.

Jarvis, N., Larsbo, M., Koetsel, J., 2017. Connectivity and percolation of structural pore networks in a cultivated silt loam soil quantified by X-ray tomography. Geoderma 287, 71–79.

Jegou, D., Cluzeau, D., Wolf, H. J., Gandon, Y., Trehen, P., 1998. Assessment of the burrow system of *Lumbricus terrestris*, *Aporrectodea giardi*, and *Aporrectodea caliginosa* using X-ray computed tomography. Biol. Fertil. Soils 26, 116–121.

Joschko, M., Diestel, H., Larink, O., 1989. Assessment of earthworm burrowing efficiency in compacted soil with a combination of morphological and soil physical measurements. Biol. Fert. Soils 8, 191–196.

Kaufmann, M., Tobias, S., Schulin, R., 2010. Comparison of critical limits for crop plant growth based on different indicators for the state of soil compaction. J. Plant Nutr. Soil Sci. 173, 573–583.

Kemper, W.D., Jolley, P., Roseneau, R.C., 1988. Soil management to prevent earthworms from riddling irrigation ditch banks. Irrig. Sci. 9, 79–87.

Klute, A., 1986. Water Retention: Laboratory Methods. In: Klute, A. (Ed.), Methods of soil analysis. Part 1: Physical and mineralogical methods, 2nd edition. American Society of Agronomy Monograph No. 28, Madison, Wisconsin, USA, pp. 635–662.

Klute, A., Dirksen, C., 1986. Hydraulic Conductivity and Diffusivity: Laboratory Methods. In: Klute, A. (Ed.), Methods of soil analysis. Part 1: Physical and mineralogical methods, 2nd edition. American Society of Agronomy Monograph No. 28, Madison, Wisconsin, USA, pp. 687–734.

Krück, S., Joschko, M., Schultz-Sternberg, R., Kroschewski, B., Tessmann, J., 2006. A classification scheme for earthworm populations (Lumbricidae) in cultivated agricultural soils in Brandenburg, Germany. J. Plant Nutr. Soil Sci. 169 (5), 651-660.

Lebert, M., Brunotte, J, and Sommer, C., 2004. Ableitung von Kriterien zur Charakterisierung einer schädlichen Bodenverdichtung entstandenen durch nutzungsbedingte Verdichtung von Böden/Regelungen zur Gefahrenabwehr, Umweltbundesamt, Berlin, 122.

Lehfeldt, J., 1988. Auswirkungen von Krumenbasisverdichtungen auf die Durchwurzelbarkeit sandiger und lehmiger Bodensubstrate bei Anbau verschiedener. Arch. Acker-Pflanzenb. Bodenk. 32, 533–539.

Lemitri, A., Gilles, C., Alabi, T., Cluzeau, D., Zirbes, I., Haubruge, E., Franics, F., 2014. Impacts of earthworms on soil components and dynamics. A review. Biotechnol. Agron. Soc. Environ. 18, 121–133.

Lipiec, J., Hatano, R., 2003. Quantification of compaction effects on soil physical properties and crop growth. Geoderma 116, 107–136.

Lipiec, J., Simota, C., 1994. Role of soil and climate factors in influencing crop responses to soil compaction in central and eastern Europe. Developm.Agric. Eng. 11, 365–390.

McKenzie, B. M., Kühner, S. MacKenzie, K., Peth, S., Horn, R., 2009. Soil compaction by uniaxial loading and the survival of the earthworm Aporrectodea caliginosa. Soil Till. Res. 104, 320–323.

Obour, P. B., Keller, T., Lamandé, M., Munkholm, L. J., 2019. Pore structure characteristics and soil workability along a clay gradient. Geoderma 337, 1186-1195.

O´Connell, D.J., 1975. The measurement of apparent specific gravity of soils and its relationship to mechanical composition and plant root growth. In: Soil physical conditions and crop production. Ministry of Agriculture, Fisheries, and Food, Technical Bulletin 29. H.M. Stat. Off., London, pp. 298–313.

Otsu, N., 1979. A treshold selection method from gray-level histograms. IEEE Trans. Syst. Man, Cybern. B, Cybern. Vol. SMC-9, No. 1, 62-66.

Pagliai, M., Pellegrini, S., Vignozzi, N., Rousseva, S., Grasselli, O., 2000. The quantification of the effect of subsoil compaction on soil property and related physical properties under conventional to reduced management practices. Adv. Geoecol. 32, 305–313.

Perreault, J.M., Whalen, J.K., 2006. Earthworm burrowing in laboratory microcosms as influenced by soil temperature and moisture. Pedobiologia 50, 397–403.

Pihlap, E., Vuko, M., Lucas, M., Steffens, M., Schloter, M., Vetterlein, D., Endenich, M., Kögel-Knabner, I., 2019. Initial soil formation in an agriculturally reclaimed open-cast mining area - the role of management and loess parent material. Soil Till. Res. 191, 224-237.

Pöhlitz, J., Rücknagel, J., Koblenz, B., Schlüter, S., Vogel, H.-J., Christen, O., 2019. Computed tomography as an extension of classical methods in the analysis of soil compaction, exemplified on samples from two tillage treatments and at two moisture tensions. Geoderma 346, 52-62.

Rabot, E. Wiesmeier, M., Schlüter, S., Vogel, H.-J., 2018. Soil structure as an indicator of soil functions. A review. Geoderma 314, 122-137.

Rasband W.S., 1997 - 2015. ImageJ. U.S. National Institute of Health, Bethesda, Maryland, USA. http://imagej.nih.gov/ij/

Rashid, S., Sheikh, K.H., 1977. Response of wheat to different levels of soil compaction. Phyton 18, 43–56.

Reichelt, J. M., Suzuki, L. E. A. S., Reinert, D. J., Horn, R., and Håkansson, I., 2009. Reference bulk density and critical degree-of-compactness for no-till crop production in subtropical highly weathered soils, Soil & Till. Res. 102, 242-254.

Renard, P., Allard, D., 2013. Connectivity metrics for subsurface flow and transport. Adv. Water Res. 51, 168-196.

Ruiz, S. Or, D., Schymanski, S., 2015. Soil Penetration by Earthworms and Plant Roots–”Mechanical Energetics of Bioturbation of Compacted Soils. PloS one 10: e0128914. 10.1371/journal.pone.0128914.

Rücknagel, J., Hofmann, B., Paul, R., Christen, O., Hülsbergen, K., 2007. Estimating precompression stress of structured soils on the basis of aggregate density and dry bulk density. Soil Till. Res. 92, 213–220.

Rücknagel, J., Brandhuber, R., Hofmann, B., Lebert, M., Marschall, K., Paul, R., Stock, O., Christen, O., 2010. Variance of mechanical precompression stress in graphic estimations using the Casagrande method and derived mathematical models. Soil Till. Res. 106, 165–170.

Rücknagel., J., Christen, O., Hofmann, B., Ulrich, S., 2012. A simple model to estimate change in precompression stress as a function of water content on the basis of precompression stress at field capacity. Geoderma 177-178, 1-7.

Rücknagel, J., Rademacher, A., Götze, P., Hofmann, B., Christen, O., 2017. Uniaxial compression behaviour and soil physical quality of topsoils under conventional and conservation tillage. Geoderma 286, 1–7.

Saqib, M., Akhtar, J., Qureshi, R. H., 2004. Pot study on wheat growth in saline and waterlogged compacted soil. I. Grain yield and yield components. Soil Till. Res. 77, 169–177.

Schjønning, P., Lamandé, M. 2018. Models for prediction of soil precompression stress from readily available soil properties. Geoderma 320, 115-125.

Schjonning, P. & Rasmussen, K. J., 2000. Soil strength and soil pore characteristics for direct drilled and ploughed soils. Soil Till. Res. 57 (1), 68-82.

Schjonning, P., van den Akker, J.J.H., Keller, T., Greve, M.H., Lamande, M., Simojoki, A., Stettler, M., Arvidsson, J., Breuning-Madsen, H., 2015. Drive-Pressure-State-Impact-Response (DPSIR) analysis and risk assessment for soil compaction – a European perspective. Adv. Agr. 133, 183–237.

Schlüter, S., Sheppard, A., Brown, K., Wildenschild, D., 2014. Image processing of multiphase images obtained via X-ray microtomography: A review. Water Resour. Res. 50, 3615-3639.

Schrader, S., Rogasik, H., Onasch, I., Jegou, D., 2007. Assessment of soil structural differentiation around earthworm burrows by means of X-ray computed tomography and scanning electron microscopy. Geoderma 137, 378–387.

Shah, A. N., Tanveer, M., Shahzad, B., Yang, G., Fahad, S., Ali, S., Bukhari, M. A., Tung, S. A., Hafeez, A., Souliyanonh, B., 2017. Soil compaction effects on soil health and crop productivity: An overview. Environ. Sci. Pollut. Res. 24, 10056–10067.

Skinner, A., Lunt, I., Spooner, P., McIntyre, S., 2009. The effect of soil compaction on germination and early growth of Eucalyptus albens and an exotic annual grass. Austral. Ecol. 34, 698-704.

Stovold, R. J., Whally, W. R., Harris, P. J., White, P. W., 2004. Spatial variation in soil compaction, and the burrowing activity of the earthworm *Aporrectodea caliginosa*. Biol. Fertil. Soil 39, 360-365.

Tursic, I., 1982. The effect of soil compaction and mineral fertilization on the yield of spring barley. Polj. Znan. Smotra-Agr. Consp. 58, 39-48 (in Croatian with an English summary).

Vogel, H.-J., Weller, U., and Schlüuter, S. 2010: Quantification of soil structure based on Minkoski functions, Computers & Geo-sciences, 36, 1236-1245.

Werner, D., Paul, R., 1999. Kennzeichnung der Verdichtungsgefährdung landwirtschaftlich genutz-ter Böden. Wasser und Boden 51, 10-14.

Witzenberger, A., Hack, H., van den Boom, T., 1989. Erläuterungen zum BBCH-Dezimal-Code für die Entwicklungsstadien des Getreides - mit Abbildungen. Gesunde Pflanzen 41, 384-388.

Table 1: Description of the sampled sites.

Site	T (°C)	N (mm)	Taxonomy[a]	Texture (g kg^{-1})		Texture class[b]	TOC (g kg^{-1})	pH	Nutrients (mg per 100 g)			N_{min} (kg N ha^{-1})	BD (Mg m^{-3})	K_s (cm d^{-1})
				Clay	Sand				P	K	Mg			
Quellendorf	8.7	526	Chernozem	130	450	loam	14	7.4	6.8	22.1	10.4	11	1.29	158
Buttelstedt	8.4	541	Chernozem	280	40	silty clay loam	21	6.9	3.5	51.3	24.1	15	1.14	157
Rothenberga	8.5	500	Haplic Luvisol	130	60	silt loam	13	6.7	5.9	19.0	6.0	17	1.10	137
Kranichborn	8.5	500	Mollic Fluvisol	70	530	sandy loam	51	7.4	12.4	13.9	12.1	30	0.82	157

T = average annual temperature; N = average annual precipitation; TOC = total organic carbon; P = phosphorus; K = potassium; Mg = magnesium; N_{min} = mineralizable nitrogen; BD = dry bulk density; K_s = saturated hydraulic conductivity

All parameters except BD and K_s were determined by Eurofins Agraranalytik Deutschland GmbH, Jena, Germany.

[a] FAO (1998)

[b] USDA classification scheme (Gee & Bauder, 1986)

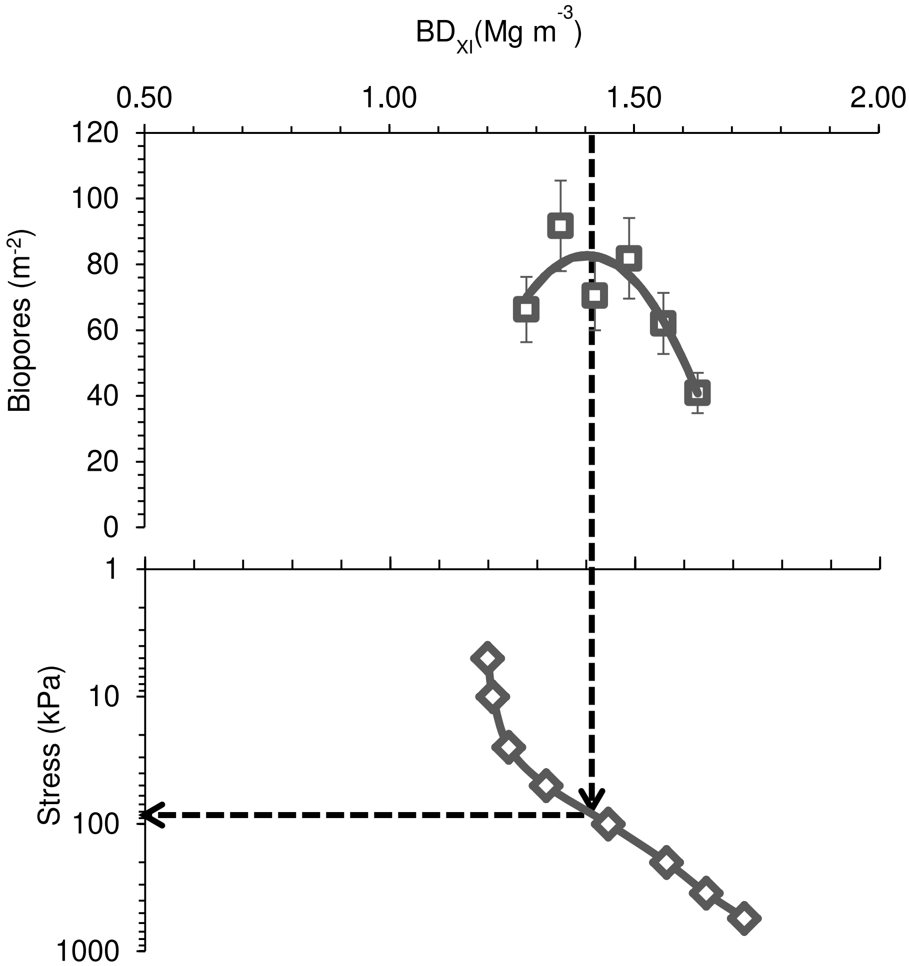

Figure 1: Scheme to derive critical stress value for earthworm activity. BD_{opt} (1.41 Mg m^{-3}) is targeted on the abscissa of the BD – Biopores diagram. Then the critical stress value (80 kPa) at which BD_{opt} value is reached can be read of the ordinate of the stress - BD_{xi} diagram.

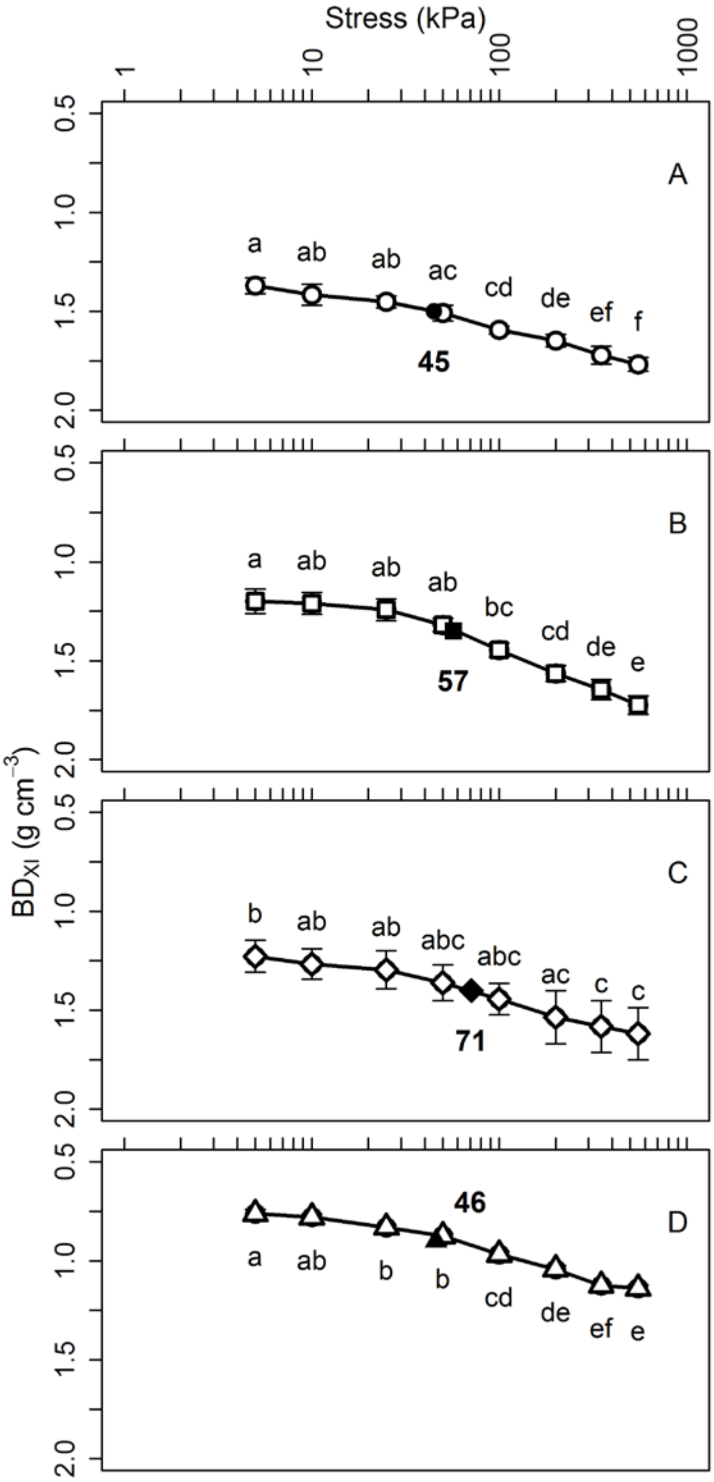

Figure 2: Dry bulk density (BD_{xi}) from sequential load application (stress) to soil cores from (A) loam, (B) silty clay loam, (C) silt loam and (D) sandy loam. Error bars show the standard deviations. Statistically significant differences ($p \leq 0.05$) are indicated by lower case letters. Black symbols and numbers indicate the values (kPa) of the mechanical pre-compression stress.

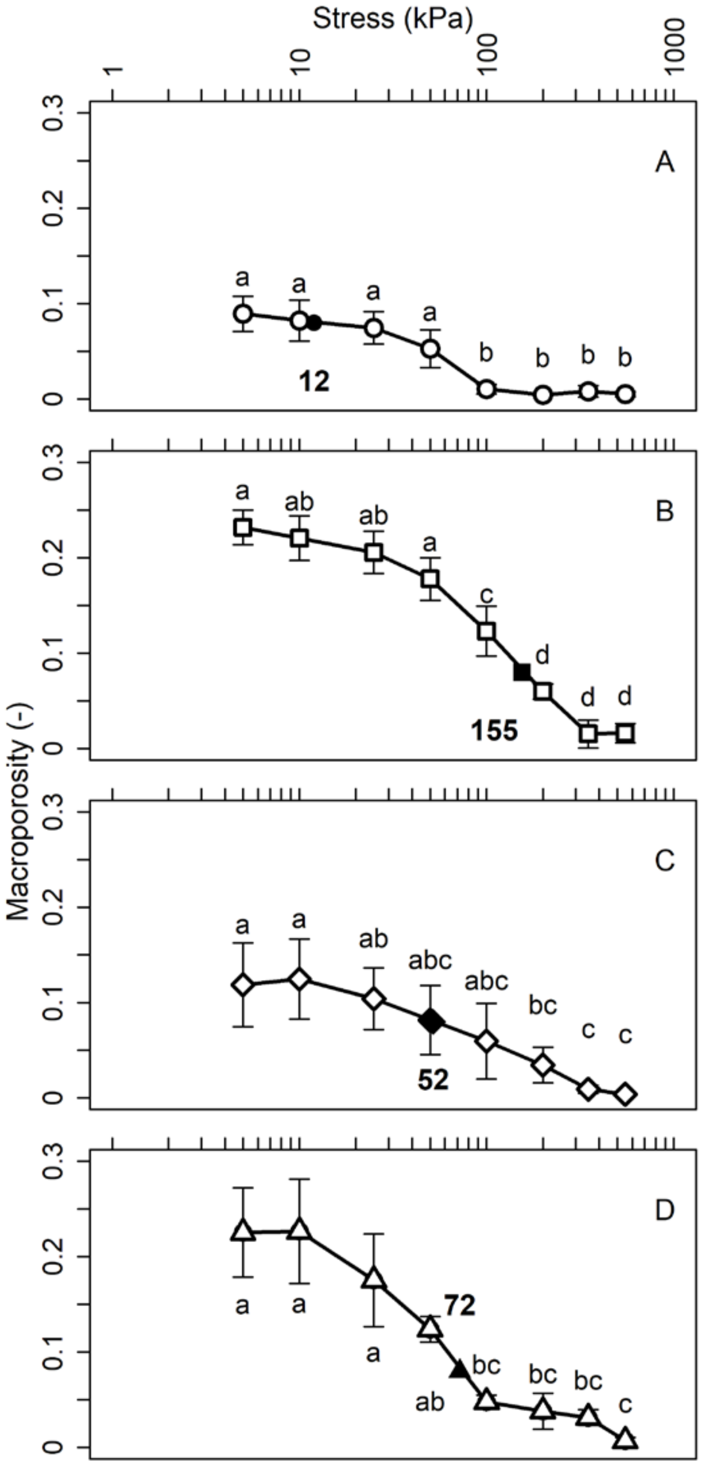

Figure 3: Macroporosity from sequential load application to soil cores for (A) loam, (B) silty clay loam, (C) silt loam and (D) sandy loam. Error bars show the standard deviations. Statistically significant differences ($p \leq 0.05$) are indicated by lower case letters. Black symbols and numbers indicate the critical stress values (kPa) which correspond to a macroporosity of 0.08.

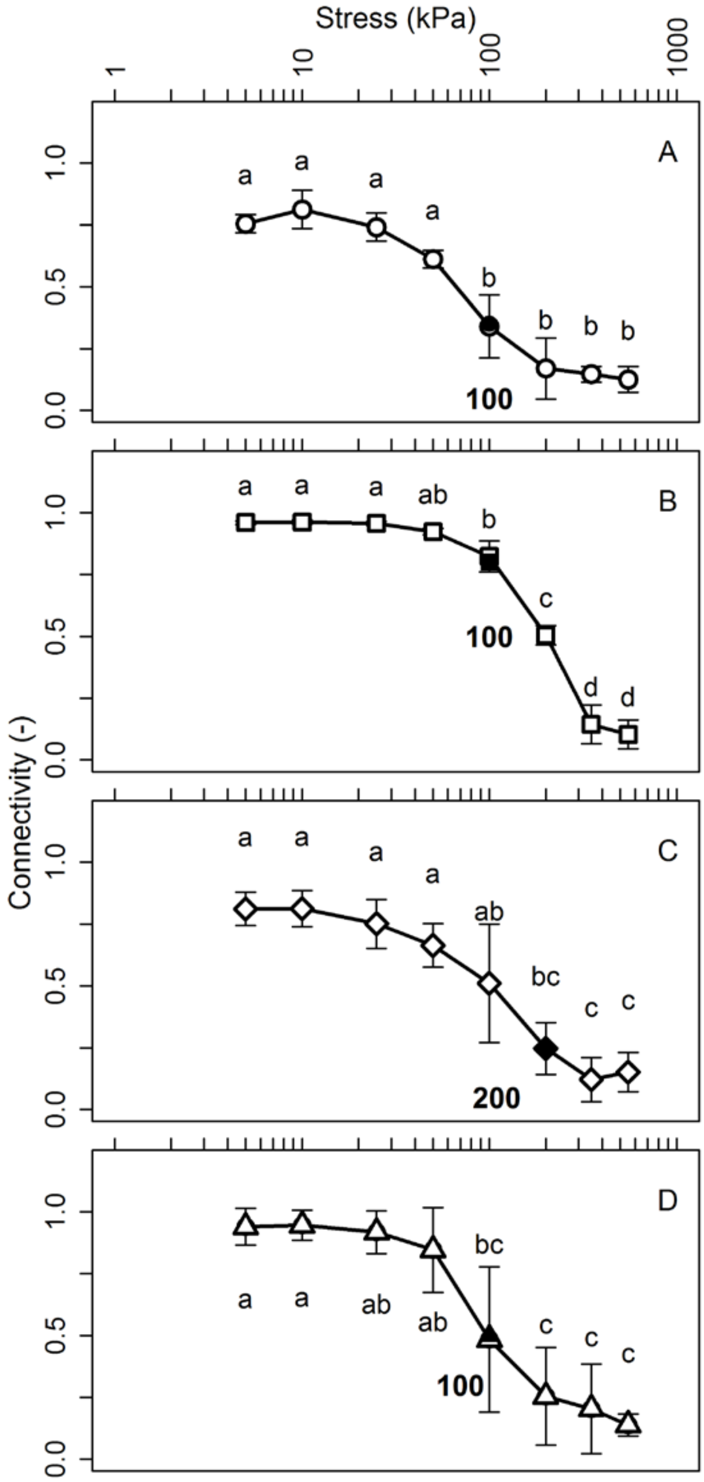

Figure 4: Pore connectivity from sequential load application to soil cores for (A) loam, (B) silty clay loam, (C) silt loam and (D) sandy loam. Error bars show the standard deviations. Statistically significant differences ($p \leq 0.05$) are indicated by lower case letters. Black symbols and numbers indicate the critical stress values (kPa) which correspond to the first significant change in pore connectivity.

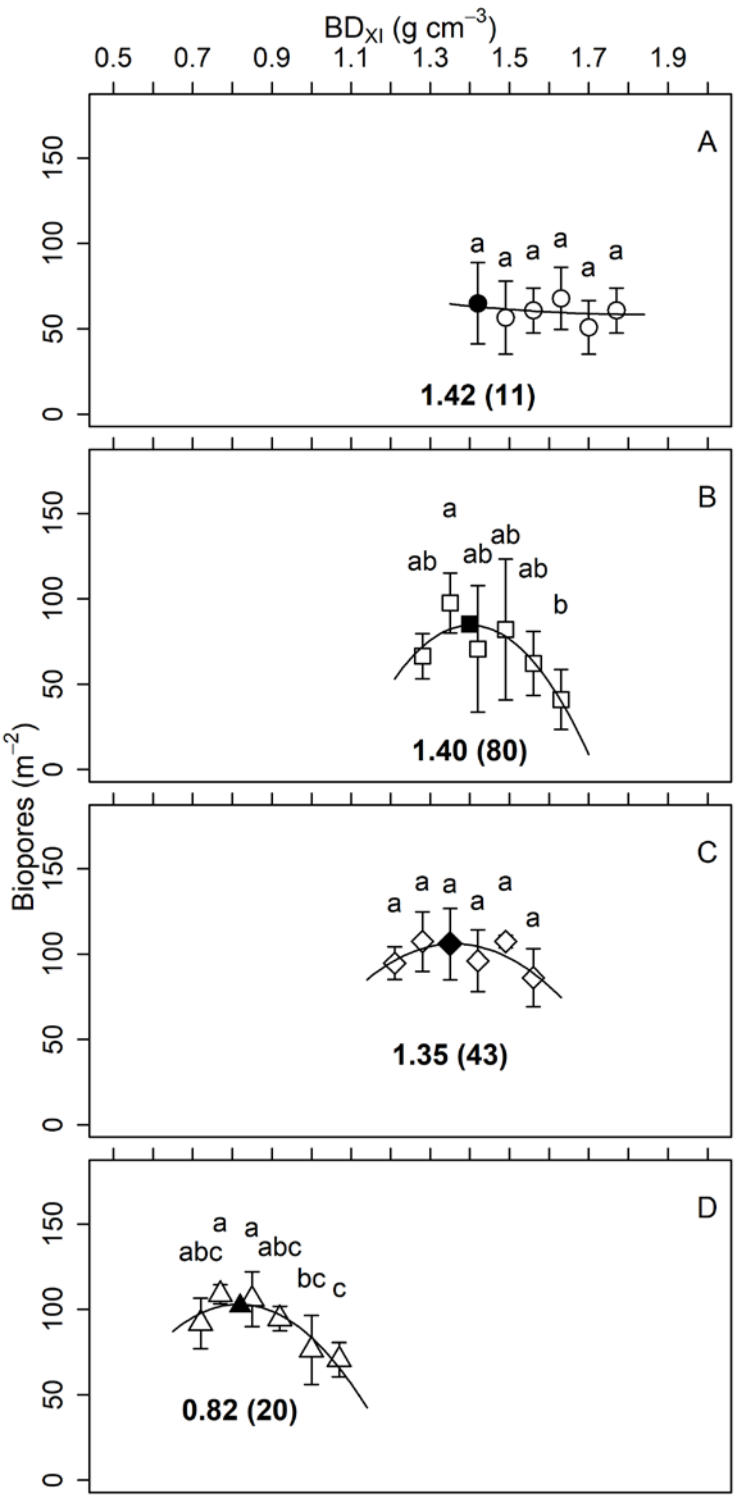

Figure 5: Biopores from *Lumbricus terrestris* as a function of dry bulk density (BD_{xi}) for (A) loam, (B) silty clay loam, (C) (silt loam and (D) sandy loam. Error bars show the standard deviations. Statistically significant differences ($p \leq 0.05$) are indicated by lower case let-

ters. Black symbols and numbers indicate the optimum BD (Mg m^{-3}) at which the biopores are at maximum and their critical stress value (kPa) in brackets.

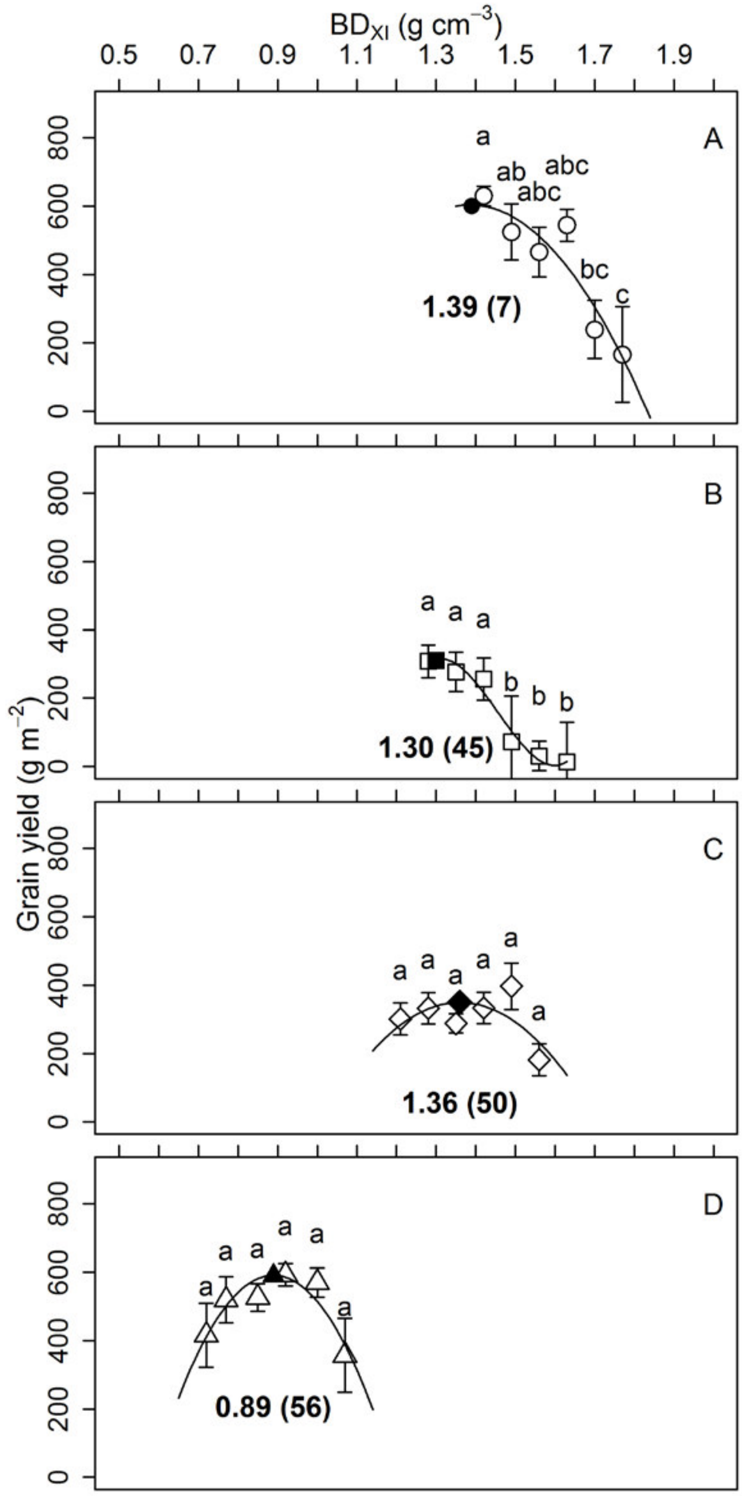

Figure 6: Grain yield of *Hordeum vulgare* as a function of dry bulk density (BD_{xi}) for (A) loam (1.42-1.77 Mg m^{-3}), (B) silty clay loam (1.28-1.63 Mg m^{-3}), (C) silt loam (1.21-

1.56 Mg m^{-3}) and (D) sandy loam (0.72-1.07 Mg m^{-3}). Statistically significant differences ($p \leq 0.05$) are indicated by lower case letters. Black symbols and numbers indicate the optimum BD (Mg m^{-3}) at which the grain yield of *Hordeum vulgare* is at maximum and their critical stress value (kPa) in brackets.

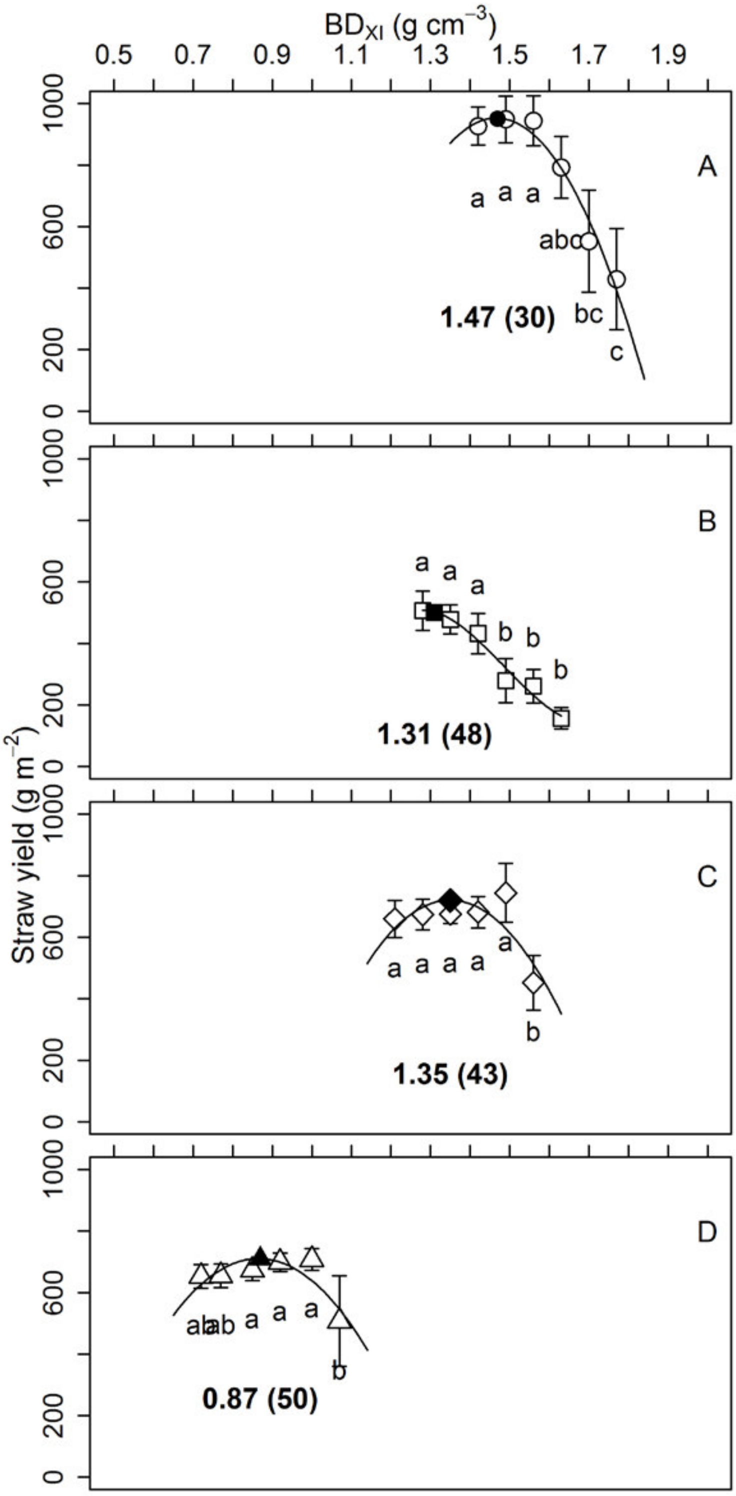

Figure 7: Straw yield of *Hordeum vulgare* as a function of dry bulk density (BD_{xi}) for (A) loam (1.42-1.77 Mg m^{-3}), (B) silty clay loam (1.28-1.63 Mg m^{-3}), (C) silt loam (1.21-1.56 Mg m^{-3}) and (D) sandy loam (0.72-1.07 Mg m^{-3}). Error bars show the standard deviations. Statistically significant differences ($p \leq 0.05$) are indicated by lower case letters. Black symbols and numbers indicate the optimum BD (Mg m^{-3}) at which the straw

yield of *Hordeum vulgare* is at maximum and their critical stress value (kPa) in brackets.

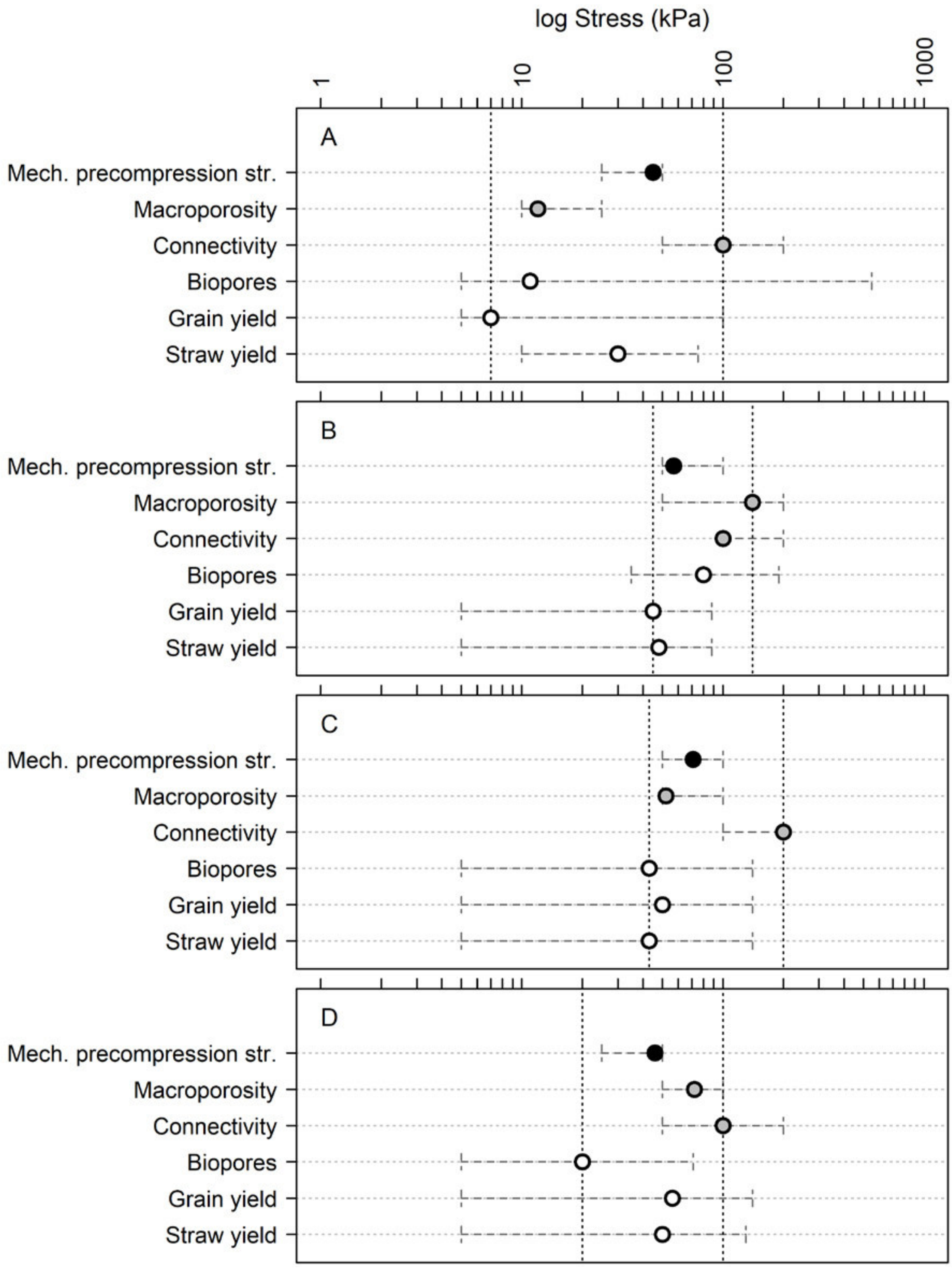

Figure 8: Critical stress ranges for (A) loam, (B) silty clay loam, (C) silt loam and (D) sandy loam based on precompression stress (black circle), critical stress values of macroporosity and pore connectivity (grey circle), and optimum values for biopores, grain yield and straw yield (white circles). The dotted vertical lines indicate the lower and upper limit of

the critical stress range for a site. The dashed horizontal lines (bars) indicate the spread (min-max) of the critical stress values among replicates for a given parameter.

Appendix 1: Examples of CT cross sectional images from load application for a load of 5, 10, 25, 50, 100, 200, 350 and 550 kPa loam (L), silty clay loam (SICL), silt loam (SIL) and sandy loam (SL).

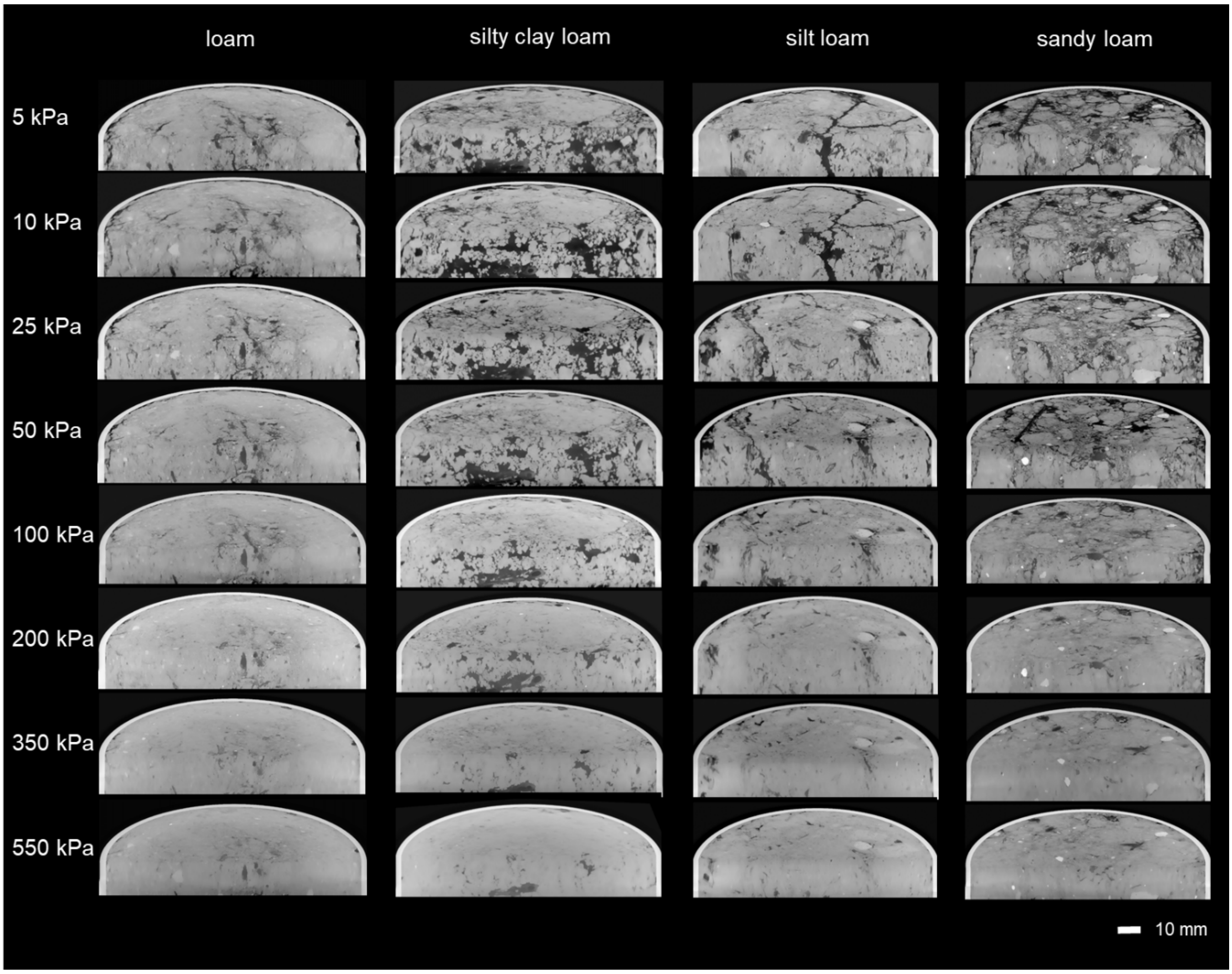

Appendix 2: Dry bulk density (BD_{xi}), macroporosity, pore connectivity, and logarithmic precompression stress ($\log \sigma_P$) for loam (L), silty clay loam (SICL), silt loam (SIL) and sandy loam (SL). Statistically significant differences ($p \leq 0.05$) are indicated by lower case (load step within each site), and upper case letters (sites within each load step).

Parameter	Texture	Load step (kPa) 5	10	25	50	100	200	350	550	$\log \sigma_P$
BD_{xi}	L	1.37 aC	1.42 abC	1.45 abC	1.51 acC	1.59 cdC	1.65 deB	1.72 efB	1.77 fB	1.65 a
($Mg\ m^{-3}$)	SICL	1.20 aB	1.21 abB	1.24 abB	1.32 abB	1.45 bcB	1.56 cdB	1.65 deB	1.72 eB	1.76 a
	SIL	1.23 bB	1.27 abB	1.30 abB	1.36 abcB	1.44 abcB	1.53 acB	1.58 cB	1.62 cB	1.85 a
	SL	0.76 aA	0.78 abA	0.83 bA	0.87 bA	0.97 cdA	1.04 deA	1.12 efA	1.14 eA	1.66 a
Macroporosity	L	0.09 aA	0.08 aAB	0.07 aA	0.05 aA	0.01 bA	0.00 bA	0.01 bB	0.01 bA	
(-)	SICL	0.23 aB	0.22 abCB	0.21 abC	0.18 aB	0.12 cB	0.06 dB	0.02 dAB	0.02 dA	
	SIL	0.12 aA	0.12 aAB	0.10 abAB	0.08 abcA	0.06 abcAB	0.03 bcAB	0.01 cAB	0.00 cA	
	SL	0.23 aB	0.23 aC	0.18 aBC	0.12 abAB	0.05 bcA	0.04 bcAB	0.03 bcAB	0.01 cA	
Pore	L	0.76 aA	0.81 aA	0.74 aC	0.61 aA	0.34 bA	0.17 bA	0.15 bA	0.13 bA	
Connectivity	SICL	0.96 aB	0.96 aB	0.96 aB	0.92 abB	0.82 bA	0.50 cB	0.14 dA	0.10 dA	

(-)	SIL	0.81 aAB	0.81 aA	0.75 aAC	0.66 aA	0.51 abA	0.25 bcAB	0.12 cA	0.15 cA
	SL	0.94 aB	0.95 aAB	0.92 abAB	0.85 abAB	0.48 bcA	0.25 cAB	0.20 cA	0.14 cA

Appendix 3: Biopores from *Lumbricus terrestris*, grain yield, straw yield, and above ground biomass of *Hordeum vulgare* for different dry bulk densities (BD) for loam (L), silty clay loam (SICL), silt loam (SIL) and sandy loam (SL). Statistically significant differences ($p \leq 0.05$) are indicated by lower case letters.

Texture	BD ($Mg\ m^{-3}$)	Biopores (m^{-2})	Grain yield ($g\ m^{2}$)	Straw yield ($g\ m^{2}$)
L	1.42	65 a	630 a	927 a
L	1.49	56 a	525 ab	949 a
L	1.56	61 a	466 abc	944 a
L	1.63	68 a	544 abc	792 abc
L	1.70	51 a	239 bc	552 bc
L	1.77	61 a	166 c	430 c
SICL	1.28	66 ab	308 a	507 a
SICL	1.35	97 a	277 a	478 a
SICL	1.42	71 ab	256 a	433 a
SICL	1.49	82 ab	72 b	279 b
SICL	1.56	62 ab	31 b	261 b
SICL	1.63	41 b	13 b	157 b
SIL	1.21	95 a	301 a	660 a
SIL	1.28	107 a	333 a	674 a
SIL	1.35	106 a	288 a	676 a
SIL	1.42	96 a	333 a	682 a
SIL	1.49	107 a	397 a	745 a
SIL	1.56	86 a	182 a	453 b
SL	0.72	92 abc	416 a	653 ab
SL	0.78	109 a	520 a	655 ab

SL	0.85	106	a	526	a	673	a
SL	0.92	95	abc	593	a	699	a
SL	1.00	76	bc	570	a	708	a
SL	1.07	71	c	357	a	508	b